EUROPEAN CONSORTIUM FOR MATHEMATICS IN INDUSTRY

ECMI Modeling Week 2019
University of Grenoble - Grenoble INP

Detection of resonances for the modelling of resonant tunneling devices

Instructor: Clément Jourdana - University of Grenoble Alpes

S. Baltieri (Università degli studi di Verona)
A. Carballosa (Universidad Autónoma de Barcelona)
M. Feder (Università degli studi di Verona)
A. Tonini (Università degli studi di Milano)
M. Zarcheva (Sofia University, "St. Kliment Ohridski")

05.09.2019

Contents

1 Introduction **3**

2 Preliminary computations **4**

2.1 Transmission coefficient **T** 4

2.2 Probability current J 5

2.3 Time-independent formulation 6

2.4 Nondimesionalization 7

3 Transparent boundary conditions: derivation and assumptions **8**

4 A finite difference approximation for the Schrödinger equation **9**

4.1 Introduction to the finite difference method 9

4.2 Application to the Schrödinger equation 10

4.3 Boundary conditions 11

4.4 Numerical illustration of the order of convergence 11

4.5 Consistency of the scheme 12

5 Implementation and strategy for energy discretization **13**

6 Numerical experiments with different potentials **14**

6.1 Variating the potential 14

7 Conclusions and perspectives **17**

7.1 Possible improvement: variational approach 18

8 Group work dynamics **19**

References **20**

1 Introduction

In Quantum mechanics, some simple unidimensional problems are the cases for a potential form of a barrier and a well, illustrated in Figure 1. For each one of these problems, one unique phenomenon occurs that is only observed in the quantum realm. In the first case, when one particle faces a potential barrier with energy lower than the height of the barrier, in the classical point of view, the particle will be reflected assuming that the impact with the barrier preserves energy and momentum. However, in quantum mechanics, the particle has a non-zero probability to appear on the other side of the barrier, since the particle does not have now a deterministic trajectory, but a density of probability of being at position x and time t distributed across a determined region of space. In this sense, the particles propagates in space according to a wave function ψ and when encountering the barrier will have a probability of being reflected and a probability of being transmitted. The latter is measured through the transmission coefficient, and the probability density in each region of the space can be computed from the Schrödinger equation (in 1D), introducing the appropiate initial and boundary conditions to account for the potential:

$$-\frac{\hbar^2}{2m}\frac{\partial^2\psi(x,t)}{\partial x^2} + V(x)\psi(x,t) = i\hbar\frac{\partial\psi(x,t)}{\partial t} \tag{1}$$

(2)

where i is the imaginary unit, m the mass, $\hbar$ the Planck constant and V is a real-valued potential

$$V(x) = \begin{cases} V_0 & \text{if } a < x < b \\ 0 & \text{elsewhere} \end{cases} \tag{3}$$

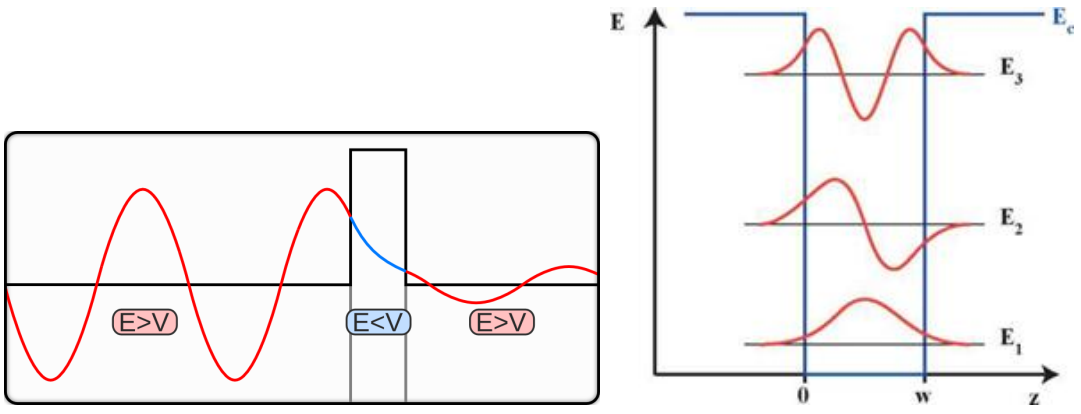

(a) (b)

Figure 1: Quantum tunneling through a potential barrier (fig a)) and a potential well with its discrete energy levels (fig b)). Figures extracted from http://elektroarsenal.net/quantum-wells.html and https://brilliant.org/wiki/quantum-tunneling/

In the problem of one particle enclosed in the quantum well, by solving Schrödinger equation one finds out that the energy states of the particle are discretized as Figure 1 shows, instead of the continuous range that one would expect in classical dynamics.

Now, here what concerns us is the interesting problem of putting together two or more potential barriers creating a quantum well in the middle. This is what occurs in the resonant tunneling devices, which receive its name because it is observed that for some incident energy of the electrons the transmission coefficient equals to 1. This is, the electrons go through the device without "seeing" the barriers. The nature of this curious effect arises from the discretization of the energy states inside the quantum well, producing that when the energy of the incident electron coincides with one of the energy levels of the well, the transmission coefficient peaks to one, as shown in Figure 2. This effect allows for an application of resonant tunneling transistors as promising switching devices, ideal for memory storing.

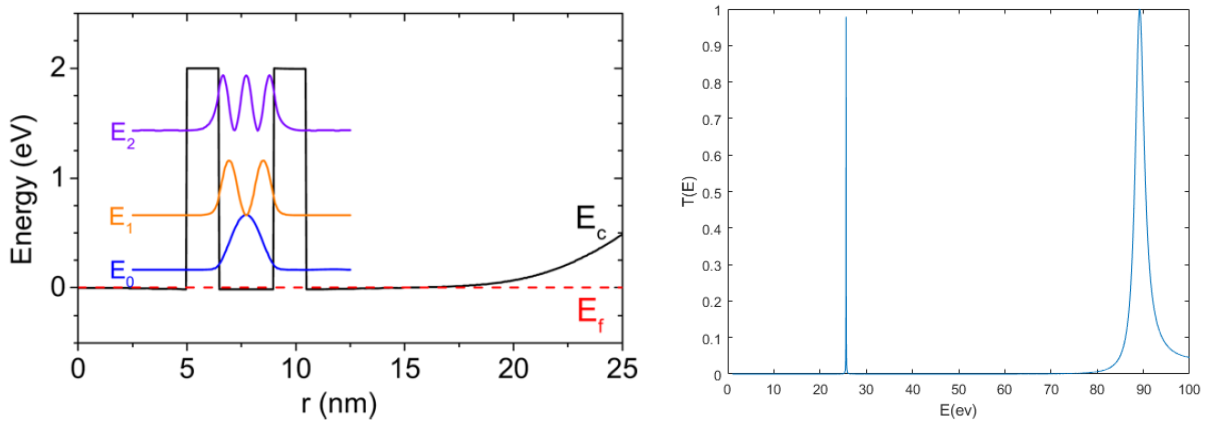

(a) (b)

Figure 2: Resonant tunneling (fig a)) and transmission coefficient (fig b)) for a double barrier. Fig. a) was extracted from http://dx.doi.org/10.1063/1.3701586

In this work, we attempt to study the problem of two or more potential barriers from a numerical point of view and in an ideal situation (with null potential difference between the extremities of the device). For this purpose, we find that the main feature of the problem is to characterize accurately the transmission coefficient in function of the incident energy, since this curve will provide all the information needed on the energy resonances and the transmission peaks. Considering that each value of the energy will imply to solve a Schrödinger equation, we must also find a strong optimization to the numerical implementation in order to reduce the computational cost, solving therefore a more reasonable number of differential equations. The optimization that we will describe here will be that of an adaptive mesh scheme in the energy discretization.

2 Preliminary computations

2.1 Transmission coefficient T

As a beginning, we will make a quick review of the process of *quantum tunneling*.

Let us consider a wave, travelling through a transmission line from a generating source towards a load. This wave becomes an *incident wave* when it meets a discontinuity or another medium with

different propagation characteristics. In this situation, some or all of the wave will be reflected back in the direction of the origin [3].

If a wave travelling within a force field reaches a region that has a potential significantly higher than the potential at the points surrounding it, we observe an incident wave upon a *potential barrier*. At the quantum level (observing particles and energies on subatomic scale), it is possible for a particle to pass trough the barrier, without having the potential energy required. This phenomenon is known as *quantum tunnelling*.

The quantity that describes the probability of a particle tunneling through a barrier is the so called *transmission coefficient*. By definition, the *transmission coefficient* T is described by the following ratio:

$$T = \frac{J_{trans}.\overline{n}}{J_{inj}.\overline{n}},$$

where J_{inj} is the *probability current* in the wave incident upon the barrier with normal unit vector $\overline{n}$, and J_{trans} is the *probability current* in the wave that has passed on the other side of the barrier [4].

In the following section, we will introduce the concept of *probability current*.

2.2 Probability current J

Probability current (probability flux) is a formalism in quantum mechanics that describes the flow of probability. It is defined as the probability per unit time, per unit area. We need to establish a connection between the variables in the model and the unknown probability flux in order to compute the transmission coefficient T.

It is not a coincidence that the quantity of interest is called probability *flux*. When talking about flux, the first thing to come in mind is the continuity equation. It appears that there is a conserved quantity in the process, that is, the *probability density* and we can obtain the definition of probability flux, using it [5]. If one thinks about the *probability density* as a heterogeneous fluid, then the *probability current* is the rate of flow of this fluid [6].
The *probability density* is defined as

$$P(x,t) = |\psi|^2 = \psi^*(x,t)\psi(x,t),$$

where ψ^* is the complex conjugate of ψ.

Differentiating it with respect to time, we obtain

$$\frac{\partial}{\partial t}P(x,t) = \left[\frac{\partial \psi^*}{\partial t}\psi + \psi^*\frac{\partial \psi}{\partial t}\right]. \tag{4}$$

Using the Schrödinger equation for ψ and its complex conjugate, multiplying them for ψ^* and ψ respectively, we obtain

$$\psi^* \left(\mathbf{i}\hbar \frac{\partial \psi}{\partial t} \right) = \left(-\frac{\hbar^2}{2m} \frac{\partial^2 \psi}{\partial x^2} + V(x)\psi \right) \psi^*$$

$$\psi \left(-\mathbf{i}\hbar \frac{\partial \psi^*}{\partial t} \right) = \left(-\frac{\hbar^2}{2m} \frac{\partial^2 \psi^*}{\partial x^2} + V(x)\psi^* \right) \psi$$

Using these expression into (4), it leads to

$$\begin{aligned} \frac{\partial}{\partial t} P(x,t) =& \frac{1}{\mathbf{i}\hbar} \left[\frac{\hbar^2}{2m} \frac{\partial^2 \psi^*}{\partial x^2} \psi - \cancel{V(x)\psi^*\psi} - \frac{\hbar^2}{2m} \frac{\partial^2 \psi}{\partial x^2} \psi^* + \cancel{V(x)\psi^*\psi} \right] \\ =& \frac{\hbar}{2m\mathbf{i}} \frac{\partial}{\partial x} \left[\frac{\partial \psi^*}{\partial x} \psi - \psi^* \frac{\partial \psi}{\partial x} \right]. \end{aligned}$$

We define $j(x,t)$ as the *probability current*:

$$j(x,t) = \frac{\hbar}{2m\mathbf{i}} \left[\psi^* \frac{\partial \psi}{\partial x} - \frac{\partial \psi^*}{\partial x} \psi \right] = \frac{\hbar}{m} Im \left(\psi^* \frac{\partial \psi}{\partial x} \right). \tag{5}$$

We have just derived the probability conservation equation

$$\frac{\partial P(x,t)}{\partial t} + \frac{\partial j(x,t)}{\partial x} = 0. \tag{6}$$

Now, we can use (5) to compute the transmission coefficient.

2.3 Time-independent formulation

The time-dependent Schrödinger equation predicts that wave functions can form stationary states, called standing waves. In physics, a standing wave (stationary wave) is a wave which oscillates in time but whose peak amplitude profile does not move in space. The peak amplitude of the wave oscillations at any point in space is constant with time. This phenomenon usually occurs as a result of interference between two waves traveling in opposite directions, for example in the case of resonance [7].

Such stationary state is an eigenvector of the Hamiltonian. It means, that we are observing a situation where the system has a single definite energy (instead of a quantum superposition of different energies). It is also called *energy eigenvector*.

For a single-particle Hamiltonian, a stationary state means that the particle has a constant probability distribution for its position, its velocity, its spin, etc. (this is true assuming that the Hamiltonian is unchanging in time). We should note that the wavefunction itself is not stationary, which is the case we consider in this report since the potential V is assuming to be independent of the time [7].

These states are particularly important as their individual study later simplifies the task of solving the time-dependent Schrödinger equation for any state. Stationary states can be described by the time-independent Schrödinger equation.

The time-independent formulation can be obtained using the classical method of separation of variables, as following

Let

$$\psi(x,t) = \varphi(x)f(t)$$

Then, equation (1) writes

$$\mathbf{i}\hbar\varphi(x)\frac{df(t)}{dt} = -\frac{\hbar^2}{2m}\frac{d^2\varphi(x)}{dx^2}f(t) + V(x)\varphi(x)f(t)/.\frac{1}{\varphi(x)f(t)}$$

Dividing by $\varphi(x)f(t)$, we obtain

$$\frac{1}{f(t)}\mathbf{i}\hbar\frac{df(t)}{dt} = -\frac{\hbar^2}{2m}\frac{1}{\varphi(x)}\frac{d^2\varphi(x)}{dx^2} + V(x) = const. = E.$$

Multiplying by $\varphi(x)$ the space equation, it gives the time-independent Schrödinger equation

$$-\frac{\hbar^2}{2m}\frac{d^2\varphi(x)}{dx^2} = (E - V(x))\varphi(x), \tag{7}$$

where E represents the particle energy.

2.4 Nondimesionalization

Before to start with the numerical computations, what we can notice, is that some very small numbers appear in equation (7)

$$\frac{\hbar^2}{m} = \frac{(1.054571726\cdot 10^{-34}Js)^2}{9.109383702\cdot 10^{-31}kg} \approx 1.220852652\cdot 10^{-38}\frac{J^2s^2}{kg} \approx 4.756006764\cdot 10^{-1}\frac{eV^2s^2}{kg}$$
$$1eV = 1.602176634\cdot 10^{-19}J$$

Moreover, for quantum devices, the length of the domain is small (of the order of nanometers). In order to avoid computations with such small numbers, we shall derive a non-dimensional form of the model. For this purpose, we use the following change of variables:

$$\overline{x} = \frac{x}{\lambda} \qquad \widetilde{V} = \frac{V(\overline{x})}{E_c} \qquad \widetilde{E} = \frac{E(\overline{x})}{E_c}$$

$$E_c := \frac{\hbar^2}{m\lambda^2} \qquad [E_c] = ML^{-2}T^{-2},$$

with λ-characteristic length, which is usually set to be the length of the domain of interest, and E_c the characteristic energy.
Making a substitution in (7), we obtain

$$\frac{1}{2}\frac{d^2\varphi}{d\overline{x}^2} = (\widetilde{V}(\overline{x}) - \widetilde{E})\varphi(\overline{x}) \tag{8}$$

From now on, all the experiments in the report are derived using (8).

3 Transparent boundary conditions: derivation and assumptions

Following [2] we assume that the access zones are $(-\infty, 0)$ and $(1, +\infty)$. Those zones are waveguides in which the potential is assumed to be constant. Then we can solve the Schrödinger equation in such regions, and we reduce our problem just to the interval $(0, 1)$. The main problem is that we do *not* know the wave function at the new boundaries $x = 0$ and $x = 1$, therefore boundary conditions have to be derived. For that, we assume an electron wave with a wavevector $k > 0$ is injected at $x = 0$. As we can see from figure (3), the waves can be transmitted at $x = 1$, or be reflected by the potential at $x = 0$. In a similar way, electrons could be injected at $x = 1$ and either transmitted at $x = 0$ or reflected at $x = 1$ (wavevector $k < 0$) but this way is not considered in this report.

Since access zones are waveguides, we assume that $V(x) = V(0) = V_0$ for $x < 0$ and $V(x) = V(1) = V_1$ for $x > 1$ and we can solve the equation (8) explicitely in those regions.

We have, for $x < 0$

$$\varphi(x) = e^{\mathbf{i}kx} + r(k)e^{-\mathbf{i}kx}$$
$$\varphi'(x) = \mathbf{i}ke^{\mathbf{i}kx} - \mathbf{i}kr(k)e^{-\mathbf{i}kx}$$

where $r(k)$ is the reflection coefficient and the relation between the energy E and the wavevector k is given by $k = 2\sqrt{E + V_0}$. It's easy to see that

$$\mathbf{i}k\varphi(0) + \varphi'(0) = [2\mathbf{i}ke^{\mathbf{i}kx}]_{x=0} = 2\mathbf{i}k$$

and leads to the boundary condition

$$\mathbf{i}k\varphi(0) + \varphi'(0) = 2\mathbf{i}k \tag{9}$$

Note that at this point everything is known, even if we do not know explicitly $r(k)$. A same argument applies to $x = 1$ and leads to the boundary condition

$$\varphi'(1) - \mathbf{i}k_2\varphi(1) = 0 \tag{10}$$

where k_2 is given by $k_2 = \sqrt{k^2 + 2(V(0) - V(1))}$

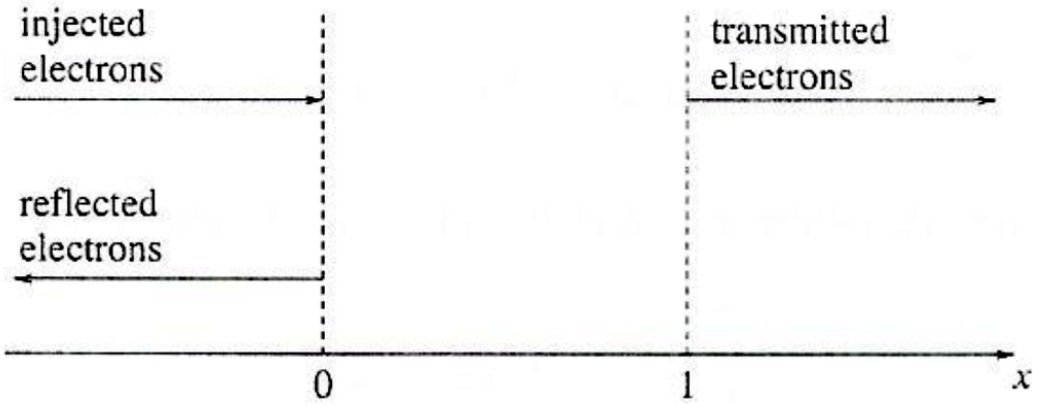

Figure 3: Electrons are injected at $x = 0$ and either reflected ($x = 0$) or transmitted at $x = 1$

4 A finite difference approximation for the Schrödinger equation

4.1 Introduction to the finite difference method

Consider the problem of approximating the derivative of a function f in an interval $[a, b]$. A natural way to proceed is to introduce N nodes in $[a, b]$ $x_k, k = 1, \ldots, N$ with $x_1 = a$, $x_N = b$ and $x_{k+1} = x_k + h, k = 1, \ldots, N - 1$, where $h = \frac{b-a}{N-1}$. Fixed x_i, we approximate $f'(x_i)$ with he value of the node $f(x_k)$ in the following way:

$$h \sum_{k=-m}^{m} \alpha_k u_{i-k} = \sum_{k=-m}^{m} \beta_k f(x_{i-k}), \tag{11}$$

where $\{\alpha_k\}_{k=-m}^{k=m}, \{\beta_k\}_{k=-m}^{k=m} \subseteq \mathbb{R}$. We note that after setting the coefficients $\{\alpha_i\}$ and $\{\beta_i\}$, to determine the values u_i, with $i \in \{1, \ldots, N\}$, it is necessary to solve a linear system.

In the case of classical finite differences, the intrinsic definition of derivative is used:

$$f'(x_i) = \lim_{h \to 0^+} \frac{f(x_i + h) - f(x_i - h)}{2h}. \tag{12}$$

By replacing the limit operation with the incremental relationship with h finite, we get the following approximation:

$$u_i = \frac{f(x_{i+1}) - f(x_{i-1})}{2h}, \quad 2 \leq i \leq N - 1. \tag{13}$$

The second member of (13) is called *centered finite difference* and corresponds geometrically to have replaced $f'(x_i)$ with the angular coefficient of the line passing through the points $(x_{i-1}, f(x_{i-1}))$ e $(x_{i+1}, f(x_{i+1}))$. Using Taylor series development, we get

$$f'(x_i) - u_i = -\frac{h^2}{6} f'''(\xi_i). \tag{14}$$

where ξ_i is a point between x_i and x_{i+1}. Then (13) is second order approximation with respect to h.

4.2 Application to the Schrödinger equation

We discretize our domain $\overline{\Omega} = [0, 1]$ with N points and the uniform mesh is made by $N - 1$ intervals of length $h = \frac{1}{N-1}$.

For the sake of simplicity we consider the nondimensional time independent Schrödinger equation (8) with *transparent boundary conditions* (9), (10)

With the centered, second order, finite difference approach, the discretized equation becomes

$$\frac{\varphi_{i+1} - 2\varphi_i + \varphi_{i-1}}{h^2} + 2(E - V(x_i))\varphi_i = 0, \quad i = 1, \dots, N.$$

The new ghost nodes φ_0 and φ_{N+1} will be discussed in the next subsection. We can easily re-write the equation as a linear system using the fact that the part corresponding to the second derivative can be written as a *matrix-vector* product $A \cdot \boldsymbol{\varphi}$, where

$$A = \frac{1}{h^2} \begin{bmatrix} -2 & 1 & 0 & 0 & \dots & 0 \\ 1 & -2 & 1 & 0 & \dots & 0 \\ 0 & \ddots & \ddots & \ddots & \ddots & \vdots \\ \vdots & \ddots & \ddots & \ddots & \ddots & 0 \\ 0 & \dots & 0 & 1 & -2 & 1 \\ 0 & \dots & 0 & 0 & 1 & -2 \end{bmatrix}$$

where $\boldsymbol{\varphi}_i = \varphi(x_i)$ and the boundary conditions has still to be imposed. The above tridiagonal matrix can be easily generated with the following MatLab command:

```
A=toeplitz(sparse([1,1],[1,2],[-2,1]/(h^2),1,N))
```

Looking at the other term of the equation, one can easily see that the whole equation becomes

$$(A + B)\boldsymbol{\varphi} = \mathbf{0},$$

where $(B)_{i,j} = 2(E - V(x_i))\delta_i^j$ for $i, j = 1, \dots, N$ where δ_i^j denotes the Kronecker symbol.

4.3 Boundary conditions

We write the first boundary condition by discretizing the first derivative with a second order approximation, by introducing a *ghost node* (or virtual node) $x_0 = x_1 - h$

$$\mathbf{i}k\varphi_1 + \frac{\varphi_2 - \varphi_0}{2h} = 2\mathbf{i}k.$$

Now, we compute φ_0 as a function of φ_1, φ_2, and we put it into the first line of the discretized system, which is

$$\frac{\varphi_2 - 2\varphi_1 + \varphi_0}{h^2} + 2(E - V(x_1))\varphi_1 = 0.$$

This leads to the following first line:

$$\varphi_1\Big(\frac{2\mathbf{i}k}{h} - \frac{2}{h^2} + 2(E - V(x_1))\Big) + \frac{2}{h^2}\varphi_2 = \frac{4\mathbf{i}k}{h}.$$

This strategy preserves the second order of the numerical scheme. After these conditions we will end up with a RHS $\boldsymbol{b}$ which is zero everywhere except for the first component $\boldsymbol{b}(1) = \frac{4\mathbf{i}k}{h}$.

Finally, the linear system to solve is

$$\frac{1}{h^2}\begin{bmatrix} 2\mathbf{i}hk - 2 + 2h^2(E - V(x_1)) & 2 & 0 & 0 & \dots & 0 \\ 1 & -2 & 1 & 0 & \dots & 0 \\ 0 & \ddots & \ddots & \ddots & \ddots & \vdots \\ \vdots & \ddots & \ddots & \ddots & \ddots & 0 \\ 0 & \dots & 0 & 1 & -2 & 1 \\ 0 & \dots & 0 & 0 & 2 & 2h\mathbf{i}k_2 - 2 + 2h^2(E - V(x_N)) \end{bmatrix} \cdot \begin{bmatrix} \varphi_1 \\ \varphi_2 \\ \vdots \\ \vdots \\ \varphi_{N-1} \\ \varphi_N \end{bmatrix} = \begin{bmatrix} \frac{4\mathbf{i}k}{h} \\ 0 \\ \vdots \\ \vdots \\ \vdots \\ 0 \end{bmatrix}.$$

solved by using the default command *backslash* in MatLab, which can easily handle complex arithmetic.

4.4 Numerical illustration of the order of convergence

In order to show numerically the order of convergence, we compute

$$\sup_{i=1\dots,N} |\varphi_i - \varphi(x_i)|$$

the infinity norm of the difference between the analytical solution and the numerical one for a different number of grid points for a potential for which we are able to compute analytically the exact solution. In this test, we choose $V(x) = 50, x \in (0, 1)$. In the logarithmic scaled plot 4 we can appreciate the right order of convergence.

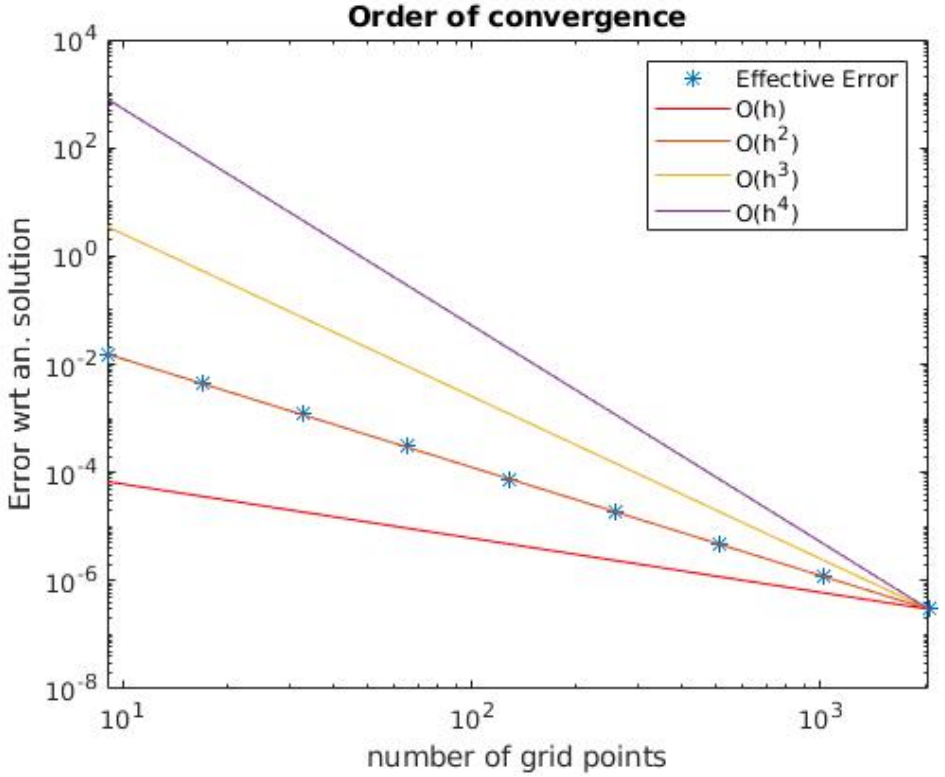

Figure 4: Order of convergence depending on the number of grid points

4.5 Consistency of the scheme

In order to show the consistency of the scheme, we insert the analytical solution $\varphi(x)$ in the numerical scheme and assuming $\varphi \in \mathcal{C}^4$, we expand in Taylor series about $x = x_i$

$$\frac{\varphi(x_{i+1}) - 2\varphi(x_i) + \varphi(x_{i-1})}{h^2} + 2(E - V(x_i)) = 0$$

and it gives, for $i = 1, \dots N - 1$

$$\varphi''(x_i) + 2(E - V(x_i)) + \varphi^{(4)}(\xi)\frac{h^2}{12} + \mathcal{O}(h^4), \quad \xi \in (x_{i-1}, x_{i+1}).$$

Since $\varphi(x)$ is the analytical solution of (8), it just remains $\varphi^{(4)}(\xi)\frac{h^2}{12} + \mathcal{O}(h^4), \quad \xi \in (x_{i-1}, x_{i+1})$.

5 Implementation and strategy for energy discretization

Now we describe the code. First of all we set the constants, the potential and the space interval. We need to find the energy levels where the resonance is. We will use a space uniform mesh to approximate the probability density function for fixed level of energy using the method described previously after the nondimensionalization. We set an energy uniform mesh, we find the approximate solutions for the different energy levels and we compute the transmission coefficients for these energy values. Then we refine uniformly the mesh used (e.g. dividing by 2 the length of the energy subintervals because we don't want to increase too much the computational cost) and we compute the new approximate solutions and transmission coefficients. Now we need to locate the energy regions where the resonance could be. We compare the transmission coefficients of the actual energy mesh and the previous one. In the previous mesh we have less values of energy for which the transmission coefficient is computed, so we need more values for the previous transmission coefficients. We used a linear interpolation to compute the transmission coefficient for the missing values of energy. The transmission coefficient is a number between 0 and 1 therefore the difference of the transmission coefficients could be very small, so we computed the relative error between the logarithms. For every energy value of the current mesh when the relative error is greater than a fixed tolerance we store the energy point. These levels of energy identify the regions where we need to refine the energy mesh. We have to separate the regions to detect those where the error is too high and we need to refine the energy mesh and to avoid to refine the energy mesh where it is useless. We calculated the variation of the logarithm of the actual transmission coefficient and we studied it on the energy levels found previously. When we have a peak the variation before it is positive and then negative. The region of one peak is identified by the levels of energy where the variation first is positive (to find the part of the region on the left of the peak) and then is negative (to find the part of the region on the right of the peak). When the variation from negative becomes positive the region is over. For every region we compute the error on the logarithm of the transmission coefficient and, if it is greater than another fixed tolerance, we need to refine the energy mesh in that region (e.g. dividing by 5 or 10 the energy step). Now we have constructed a new mesh that becomes the current one and the one before the refinement becomes the previous one and we repeat this procedure until a maximum number of iteration is reached or the error is below a fixed tolerance.
In the next figures we will study the behavior of the transmission coefficient and the refinement of the energy mesh of two different potentials, one on the left side with two barriers and the other one on the right side with five barriers.

In Figure 6 there are the approximations of the logarithm of the transmission coefficients after some iterations. We note that there are two peaks for the left potential and four for the right one. In Figure 7 there are the approximations of the transmission coefficients.

In Figure 8 we have on the left of the graphics the scale for the energy step represented with stars, on the right the scale for the transmission coefficient. We notice that near the peaks the energy step becomes really small.

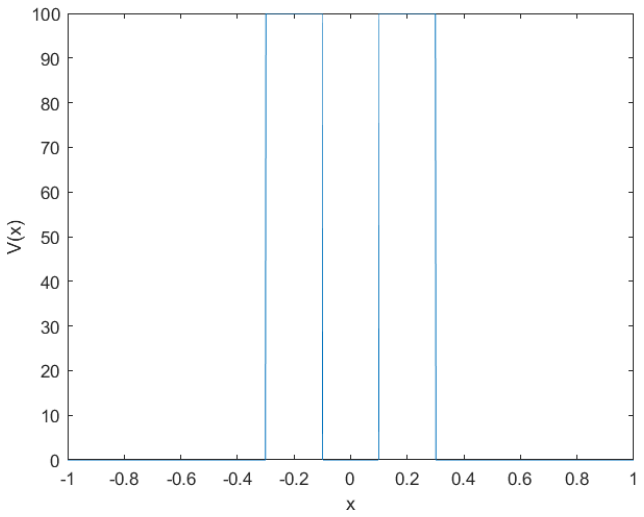

(a) 2 barriers potential

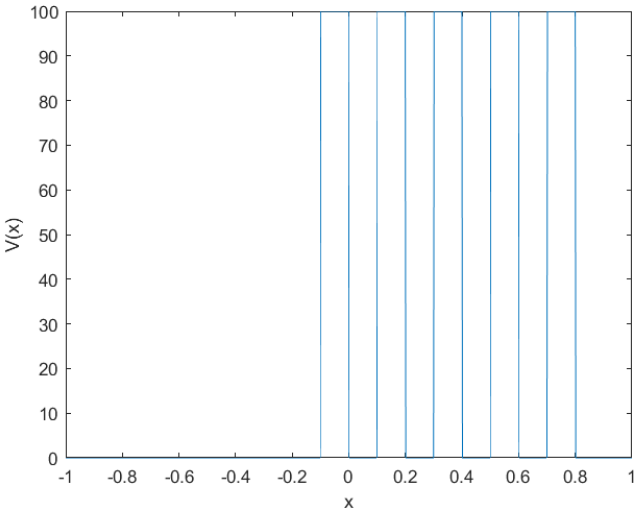

(b) 5 barriers potential

Figure 5: Potentials

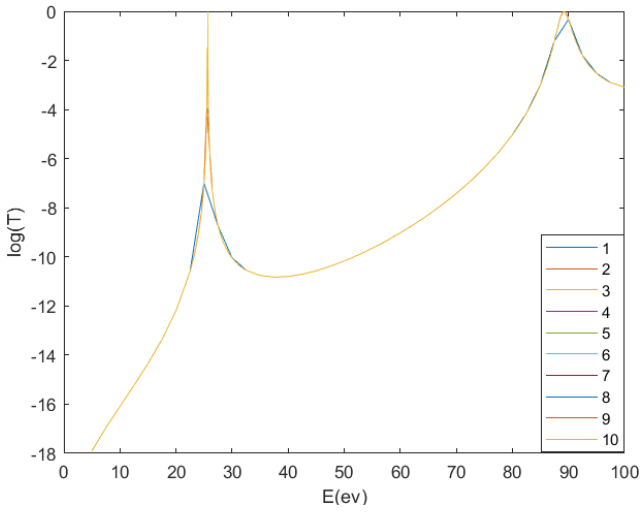

(a) 2 barriers potential

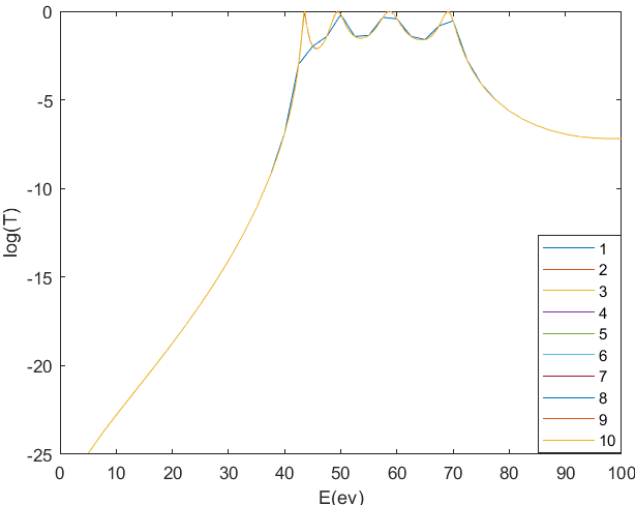

(b) 5 barriers potential

Figure 6: Approximations of the transmission coefficient at different iterations

6 Numerical experiments with different potentials

6.1 Variating the potential

Until now, we have tested identical potential barriers with the same value and ratio of width barrier/well. An important test now is to check if the optimization depends on the form of the potential. In Figure 9 we show the tested modified potentials and in Figure 10 and Figure 11 the results.

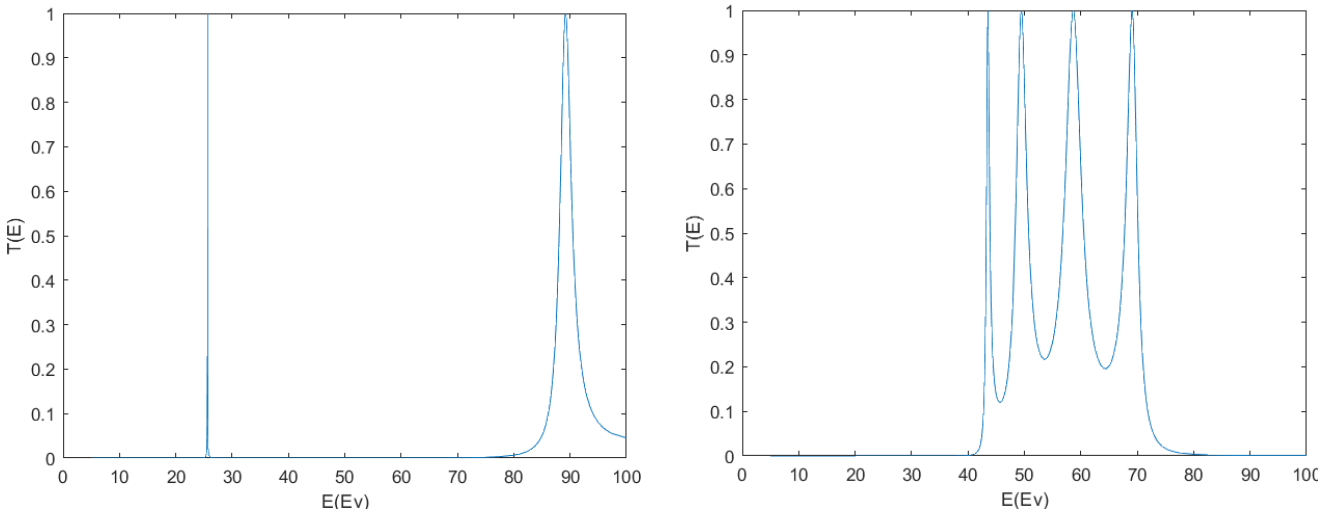

(a) 2 barriers potential

(b) 5 barriers potential

Figure 7: Transmission coefficient

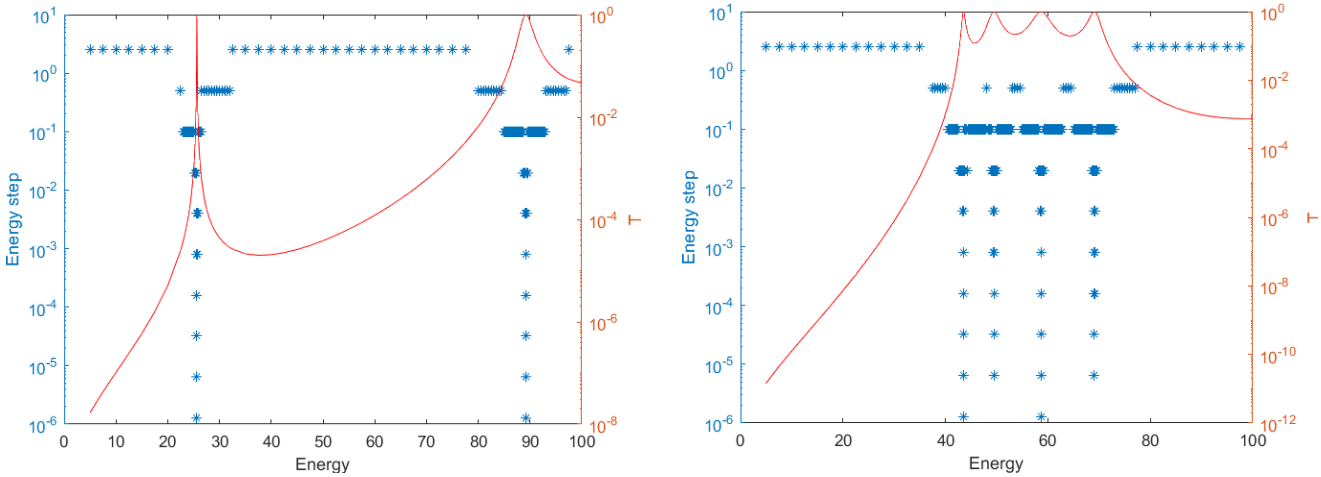

(a) 2 barriers potential

(b) 5 barriers potential

Figure 8: Mesh refinement and transmission coefficient

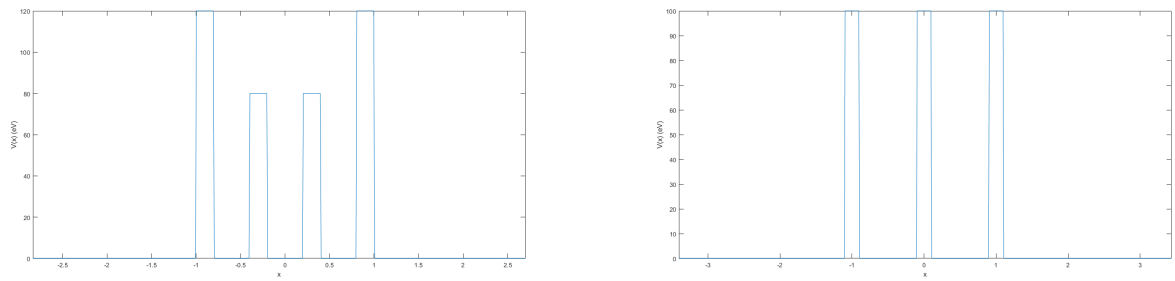

(a) Modified 4 barrier potential

(b) Modified 3 barrier potential

Figure 9: Tested modified potentials. On one hand we tried modifying the heights of the intermediate potentials and on the other we increased the weidth of the quantum wells, with 3 barriers.

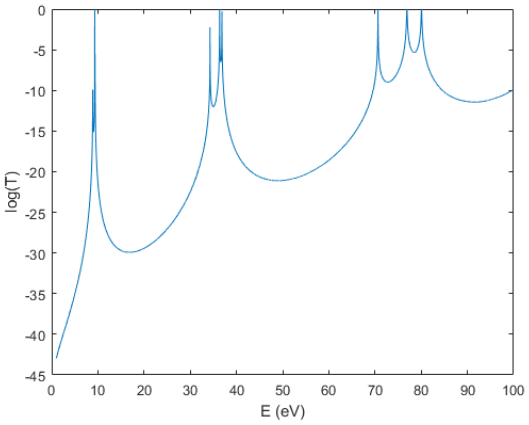

(a) $log(T)$ for the baseline code

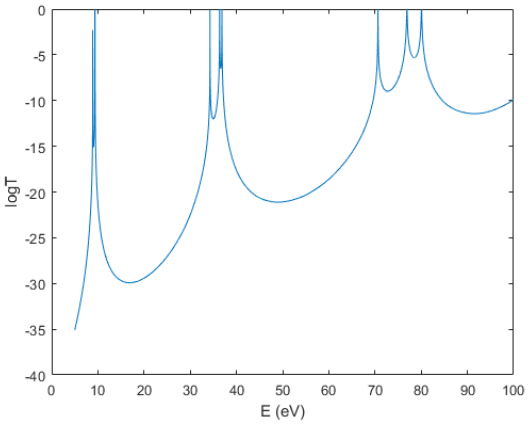

(b) $log(T)$ for the optimized code

Figure 10: Test of the optimized code for the modified 4 barriers potential

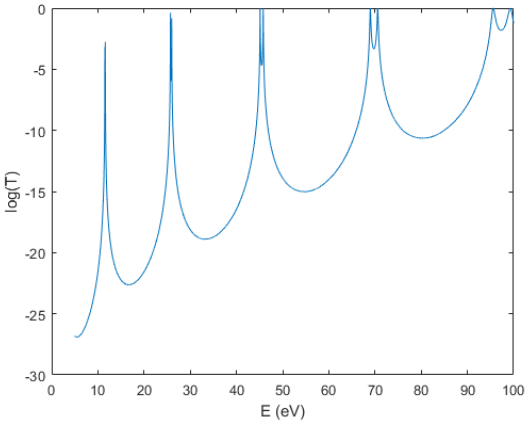

(a) $log(T)$ for the baseline code

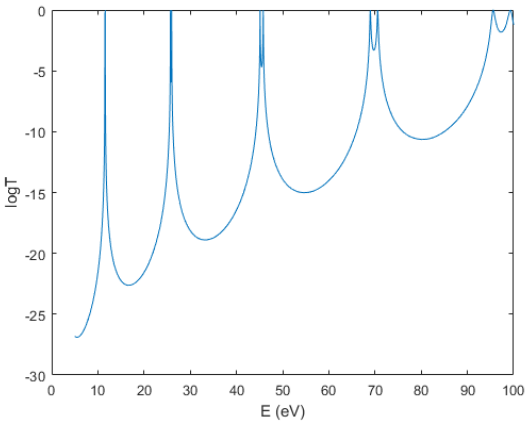

(b) $log(T)$ for the optimized code

Figure 11: Test of the optimized code for the modified 3 barriers potential

From the figures we can appreciate that our optimization passed correctly the presented test, and also we observed that these modifications on the potential produced significant differences on the position of the transmission coefficient's peaks. What's more, from this tests we extracted some remarking features of the model that can be of high interest when building the devices. For instance, we observe that a direct relation between the number of quantum wells and the number of peaks into which the transmission peaks of the 3-barrier is splitted (this effect is better shown in Figure 12). When modifying the height of the intermediate barriers we also observed that the apparent symmetry into which the peaks are splitted is broken, as Figure 10 shows. On the other hand, when increasing the width of the wells, the number of energy states inside the well is also increased, allowing for more resonant transmission peaks. This effect is already shown in Figure 11 and is exaggerated in Figure 13.

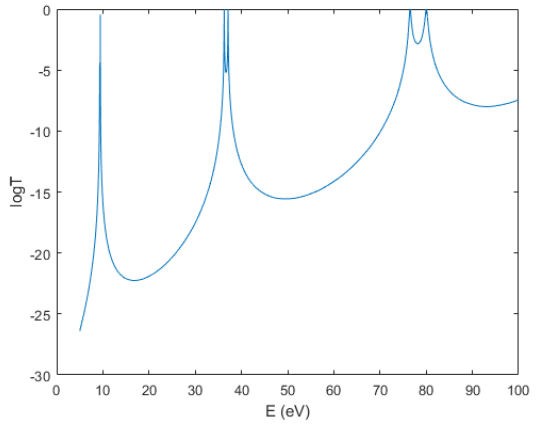

(a) Barriers=3

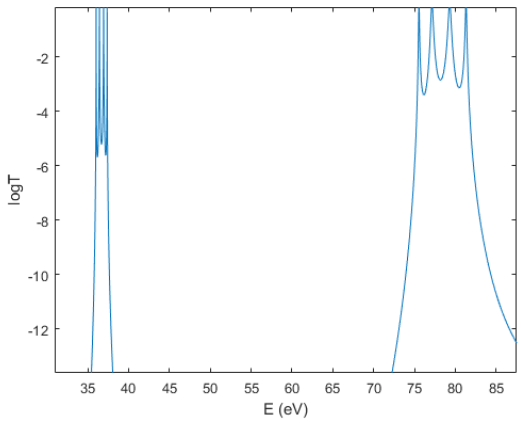

(b) Barriers=5 (zoomed)

Figure 12: Illustration of how increasing the number of barriers splits the peaks in the same amount.

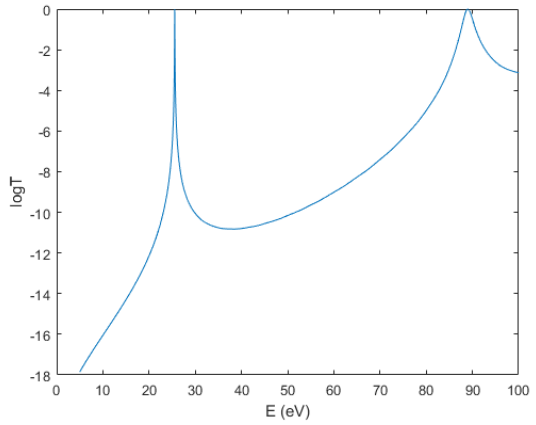

(a) Well width =0.2

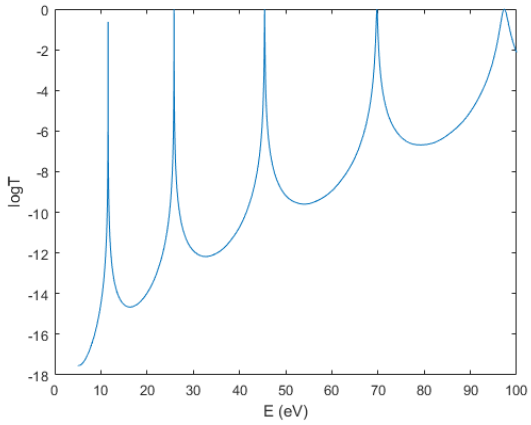

(b) Well width=0.8

Figure 13: Illustration of how increasing the width of the wells allow for more energy resonances.

7 Conclusions and perspectives

Other possible improvements can be made changing the stopping condition of the cycle in the implementation. With our code the number of iteration always reaches its maximum, but we would like that sometimes it stops before.
Every cycle we compute the solutions for every energy level of the new mesh, but for many of these levels it is useless because we have already computed the solution. At every iterations we could keep track of the solutions computed and avoid to recompute them and make the implementation quicker.
As described before, the numerical solution itself could be improved by using, for instance, a variational approach.

7.1 Possible improvement: variational approach

Since the regularity of φ strongly depends on the regularity of the potential $V(x)$, with a finite difference approach one lose the second order approximation. Indeed, with piece-wise constant potential we have no more second order approximation. This observation leads to a variational approach, requiring the solution φ to be less smooth than before.

Denoting with $H^1(0,1)$ the Sobolev space $W^{1,2}(0,1)$, as usual we take a $v \in H^1(0,1)$, multiply the equations by $\overline{v}$ and integrate by parts:

$$\int_0^1 \varphi''(x)\overline{v}(x)\mathrm{dx} + 2\int_0^1 (E - V(x))\varphi(x)\overline{v}(x)\mathrm{dx} = 0, \quad v \in H^1(0,1)$$

$$[\varphi'(x)v(x)]_0^1 - \int_0^1 \varphi'(x)v'(x)\mathrm{dx} + 2\int_0^1 (E - V(x))\varphi(x)v(x)\mathrm{dx} = 0, \quad v \in H^1(0,1)$$

Recalling that we have Robin boundary conditions, then in the weak formulation we will have terms proportional to φ. Using the fact that $\varphi'(0) = 2\mathbf{i}k - \mathbf{i}k\varphi(0)$ and $\varphi'(1) = \mathbf{i}k_2\varphi(1)$ then the weak formulation associated to (8) with boundary conditions (9)-(10) is to find $u \in H^1(0,1)$ such that

$$\mathbf{i}k_2\varphi(1)v(1) + \mathbf{i}k\varphi(0)v(0) - 2\mathbf{i}kv(0) - \int_0^1 \varphi'v'\mathrm{dx} + 2\int_0^1 (E - V(x))\varphi v\mathrm{dx} = 2\mathbf{i}k, \quad (\star)$$

holds for every $v \in H^1(0,1)$.

In order to solve it, we restrict to a proper finite dimensional subspace X_h of H^1, made by piecewise linear function, i.e. $X_h = \{w \in C^0(0,1) : w_{|[x_i,x_{i+1}]} \in \mathbb{P}([x_i, x_{i+1}])\}$. A basis of this space is given by the "hat functions" $w(x)$ and therefore we have to search for $\varphi_h \in X_h$ such that the above mentioned identity holds for every $v \in X_h$.

In particular we have

$$\varphi_h(x) = \sum_{i=1}^{N} (\varphi_h)_j w_j(x) \tag{15}$$

and the discrete problem is therefore to find $\varphi_h \in X_h$ s.t.

$$-\int_0^1 \sum_j (\varphi_h)_j w_j'(x)w_i'(x)\mathrm{dx} + 2\int_0^1 (E - V(x))\sum_j (\varphi_h)_j w_j(x)w_i(x)\mathrm{dx} + \mathbf{i}k(\varphi_h)_1 w_1 w_i(0) + ik_2(\varphi_h)_N w_N w_i(1) = 2$$

for $1 \le i \le N$

At this point one can assembly the *stiffness* matrix A, the "load" vector $\boldsymbol{b}$ and solve the linear system

$$A\boldsymbol{\varphi}_h = \mathbf{b}$$

Note that the solution of the linear system will give the coefficients φ_h of (15), not the values of φ at the nodes as in the finite difference approach.

We can also change our method to find the regions of energy refinement looking at the probability density after the first barrier of the potential. If the value of the probability is big enough something has passed through the barrier and we have to refine the energy mesh there.
Eventually we can study the behavior of the solution as time goes by computing the exact time dependent solution.

8 Group work dynamics

Most of us did not have a sufficient physical background, so we had to split the job somehow. Some of us were more practical from a numerical point of view, while others were more confident with the physics and the analysis behind the equation, so we decided to split our group in essentially two subgroups. For instance, in order to check the numerical results and see if they were reliable with the theory, we had to discuss together. We spent the first days familiarizing with the analytical and numerical solution of the equation itself, especially with the "transparent boundary conditions", since all of us were not familiar with them. After this, we checked if our numerical solution agreed with the analytical one. The remaining days we worked to the refinement of the energy, which was the main topic of the project. The time, of course, was not enough to make an optimized work, since lots of features can be improved a lot, as highlighted above.

References

[1] "Coaxial Nanowire Resonant Tunneling Diodes from non-polar AlN/GaN on Silicon", Carnevale, S.D. et al.; Appl. Phys. lett. 100, 142115 (2012)
https://arxiv.org/abs/1202.6052

[2] A. Jüngel, Transport equations for semiconductors, Lecture Notes in Physics No. 773, Springer, Berlin, 2009.

[3] Incident wave definition
https://uk.farnell.com/incident-wave-definition

[4] Transmission coefficient
https://en.wikipedia.org/wiki/Transmission_coefficient

[5] Conservation of probability
https://quantummechanics.ucsd.edu/ph130a/130_notes/node127.html

[6] Probability current
https://en.wikipedia.org/wiki/Probability_current

[7] Stationary state
https://en.wikipedia.org/wiki/Stationary_state